

**Conference Paper**

# Estimating the Ultimate Load of Cold-Formed Steel Double Lipped Channel Columns Using a Simplified Method

**Ahmed Shamel Fahmy<sup>1</sup>, Sherine Mostafa Swelem<sup>1</sup>, Rowida Saad Farrag<sup>2</sup>**<sup>1</sup>Department of Civil Engineering, Faculty of Engineering, Alexandria University, Alexandria, Egypt<sup>2</sup>Department of Constructing Engineering, Higher Institute of Engineering and Technology, Alexandria, Egypt**Email address:**

rowidafarrag@gmail.com (R. S. Farrag)

**To cite this article:**Ahmed Shamel Fahmy, Sherine Mostafa Swelem, Rowida Saad Farrag. Estimating the Ultimate Load of Cold-Formed Steel Double Lipped Channel Columns Using a Simplified Method. *Engineering Science*. Vol. 3, No. 1, 2018, pp. 1-10. doi: 10.11648/j.es.20180301.11**Received:** January 12, 2018; **Accepted:** January 30, 2018; **Published:** May 29, 2018

---

**Abstract:** A simple method is proposed to predict the ultimate load of cold formed steel lipped channel columns. The proposed method reliability based on finite element method results of the cold-formed C- channel columns under axial load [1]. Numerical investigations of buckling behavior are accomplished by using FE software ANSYS 16 [2]. A parametric study for different cross sections is carried out covering a wide range of slenderness and web depth to thickness ratio for lipped channel columns. The comparison between results obtained from the numerical method (FEM) and the proposed method is achieved to validate the precision of the simple prediction method. Finally, the proposed method is implemented on the double lipped channel columns.

**Keywords:** Cold Formed, Double Lipped Channel, Finite Element Method, Buckling, Proposed Method

---

## 1. Introduction

There are two main types of steel structural sections, namely, hot-rolled and cold-formed sections. Hot-rolled sections are quite familiar. The cold formed sections are thinner than hot-rolled sections so it can be subjected to different modes of failure and deformation [3]. Cold-formed steel products are extremely utilized in building constructions as structural members, walls, floors and roofs. There are many types of cold-formed shapes available as structural members and these types include open sections, closed sections and built-up sections [4]. These structural shapes can be used in buildings as eave struts, purlins, girts, studs, headers, floor joists, braces and other secondary building elements [5]. One of the biggest difficulties facing cold-formed steel design is the prevention of member buckling. Because of the small thickness to width ratio, it is likely that the members will buckle at compressive stresses that are lower than the yield stress. Therefore, buckling is a mainly consideration in the design of cold-formed steel members [6]. One of the three basic types of buckling which are, local, distortional and overall buckling can occur in thin-walled steel open sections. Buckling modes can occur separately or interact with each other depending on the cross-sectional dimensions and length

of the member.

In previous work [7], the finite element model is used to simulate the previous experiments [8-10]. A nonlinear finite element modelling analysis is carried out and verified using previous experimental results to study the behavior of buckling. The ultimate load, total deformation and the stress distribution obtained from ANSYS are compared with the previous experimental result to verify of the finite element technique. This model could be used in a parametric study for different cross sections. Furthermore, an extensive parametric study is performed to analyze the performance of 215 different lipped channel columns under axial pure compression. The parametric study is carried out to investigate the influences of the cross section properties of the cold-formed steel lipped channel columns on buckling behavior. The cross section selection is based on the main factors affecting the buckling behavior according to Egyptian specifications code [11].

## 2. Limitations of the Cross Sectional Dimensions

All models have a web depth (b), flange width (a) and lipped depth (c) as shown in Figure 1.

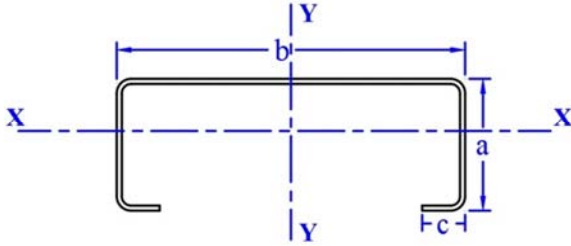


Figure 1. Simple lipped channel section.

Models are selected based on the main conditions presented in the Egyptian specification code:

1. Web depth to thickness ratio ( $b/t$ )  $\leq 300$ .
2. The flange width to thickness ratio ( $a/t$ ) and lip width to thickness ( $c/t$ ) are chosen less than 60 and 40 respectively.
3. The thickness of models is not more than 8 mm.
4. The slenderness ratio ( $\lambda$ ) doesn't exceed 180.

Five parameters ( $L$ -  $a$ -  $b$  -  $c$  -  $t$ ) affect the behavior of buckling. Table 1 illustrates the range of usage values in all models.

Table 1. Parameters values.

L (mm)	b (mm)	a (mm)	c (mm)	t (mm)
	100			1
	120			1.2
2000	150		20	1.5
2500	200	100	40	1.8
3000	250	120	60	2
3500	300	150	80	2.2
4000	350			2.5
	400			2.8
				3

### 3. Classification of Specimens

A large number of specimens are investigated to fulfill the web depth to thickness ratio ( $b/t$ ) and the slenderness ratio ( $\lambda_x$ ) simulating the performance of the structure. The slenderness ratio of member could be taken as ( $\lambda_x = L/r_x$ ) where ( $L$ ) is the unsupported length and ( $r_x$ ) is the radius of gyration. The specimens are classified to three different zones depending on its slenderness ratio. Each zone is divided into sub-zones based on the web depth to thickness ratio.

#### 3.1. Zone (1)

The slenderness ratio is less than 70. The models have different cross sectional dimensions and they make up to 53% of the total number of models. This zone is divided into two sub-zones:

##### 3.1.1. Sub-Zone (a)

The models have a web depth to thickness ratio ( $b/t$ ) that is less than 100.

##### 3.1.2. Sub-Zone (b)

The models have a web depth to thickness ratio ( $b/t$ ) more than or equal to 100.

#### 3.2. Zone (2)

The slenderness ratio lies between (70 - 120) with different values of web depth to thickness ratio. This zone contains 30% of the total number of specimens and it is divided into three sub-zones:

##### 3.2.1. Sub-Zone (c)

The models have a web depth to thickness ratio ( $b/t$ ) less than 100.

##### 3.2.2. Sub-Zone (d)

The models have a web depth to thickness ratio ( $b/t$ ) that lies between 100 to 140.

##### 3.2.3. Sub-Zone (e)

The models have a web depth to thickness ratio ( $b/t$ ) that is more than 140.

#### 3.3. Zone (3)

The slenderness ratio ranges from 120 to 180 with different values of web depth ratio. It includes 17% of the total number of models. This zone isn't divided into any sub-zones.

All zones with their sub-zones are shown in Figure 2.

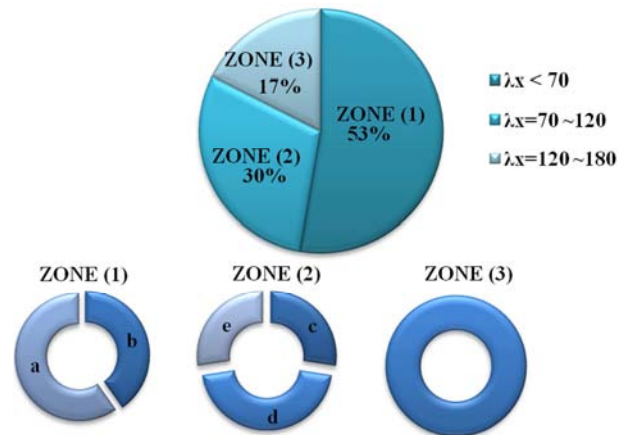


Figure 2. Classification of specimens.

### 4. Simplified Method for Predicting the Ultimate Load

A proposed method is presented to determine the ultimate loads of cold formed steel lipped channel column under pure compression. This method takes into consideration the disability of the section due to the local and overall buckling. Suitable parameters affecting the cross sections are investigated to keep the equation reliable as well as simple.

Geometrical parametric equations are derived based on all previous models using multiple nonlinear regression analysis performed by the statistical software package, "SPSS" [12]. Depending on the data obtained from the extensive analysis of parametric study, the variation of the geometrical and mechanical parameter leads to the following equation to predict the ultimate load:

$$P_p = S * (f * A) + N * (E I_x \pi^2 / L^2) \quad (1)$$

Where,

$P_p$  = predicted ultimate load in (N).

$f$  = yield stress in (N/mm<sup>2</sup>).

$A$  = cross sectional area in (mm<sup>2</sup>).

$E$  = modulus of elasticity in (N/mm<sup>2</sup>).

$I_x$  = moment of inertia about horizontal axis in (mm<sup>4</sup>).

$L$  = length of column in (mm).

$N$  and  $S$  are constants depending on columns classification.

The equation is used for all zones and sub-zones. The constants ( $S$ ,  $N$ ) vary from one zone to the other as illustrated in Table 2. The different values of constants are estimated depending on the main variables ( $f$ ,  $A$ ,  $I$  and  $L$ ) and the values of loads  $P_{(ANSYS)}$  obtained from FEM.

Table 2. Limitations for proposed method.

ZONE	$\lambda_x$	b/t	Proposed equation	S	N
(1)	< 70	< 100	$P_p = S * (f * A) + N * (E I_x \pi^2 / L^2)$	0.725	0.010
		$\geq 100$		0.300	0.030
(2)	(70-120)	< 100		0.750	-0.050
		(100-140)	0.520	-0.026	
		> 140	0.240	-0.010	
(3)	(120-180)	-----		0.200	1.200

The values of constants reflect the effect of the local and global buckling on the columns with 85% confidence interval. The proposed method is applied to all previous specimens in the different zones and sub-zones. The results calculated from the proposed method are compared with the ones obtained from (FEM) to show the accuracy of the above mentioned proposed method.

### 5. Numerical Verification

The values of ultimate loads for all the previous specimens are estimated by using the proposed method. Every zone contains different types of failure buckling moods. The section

below gives a comparison between ( $P_p$ ) from proposed method and ( $P_{ANSYS}$ ) calculated for the same specimens using (FEM) as follows:

#### 5.1. Numerical Verification of Zone (1)

Most of the specimens in sub-zone (a) are subjected to distortional buckling. In sub-zone (b) most of the models are subjected to flexural buckling. Figure 3 presents the comparison between results obtained from the simplified method ( $P_p$ ) and the previous results obtained from finite element method ( $P_{ANSYS}$ ).

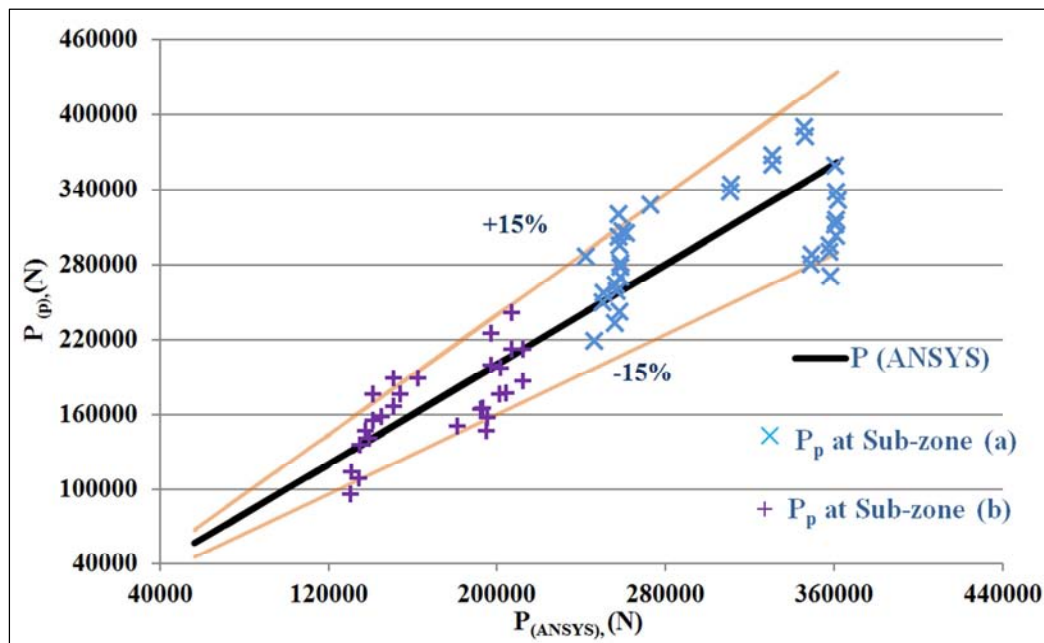


Figure 3. Results of ultimate load in zone (1).

#### 5.2. Numerical Verification of Zone (2)

In all sub-zones (c) (d) and (e) most of the models undergo local buckling. The variable dimensions lead to different type of deformations. As a result the constants of the equation ( $S$ ,  $N$ ) have a different value in each sub-zone. Figure 4 presents the comparison between ultimate loads obtained from both methods.

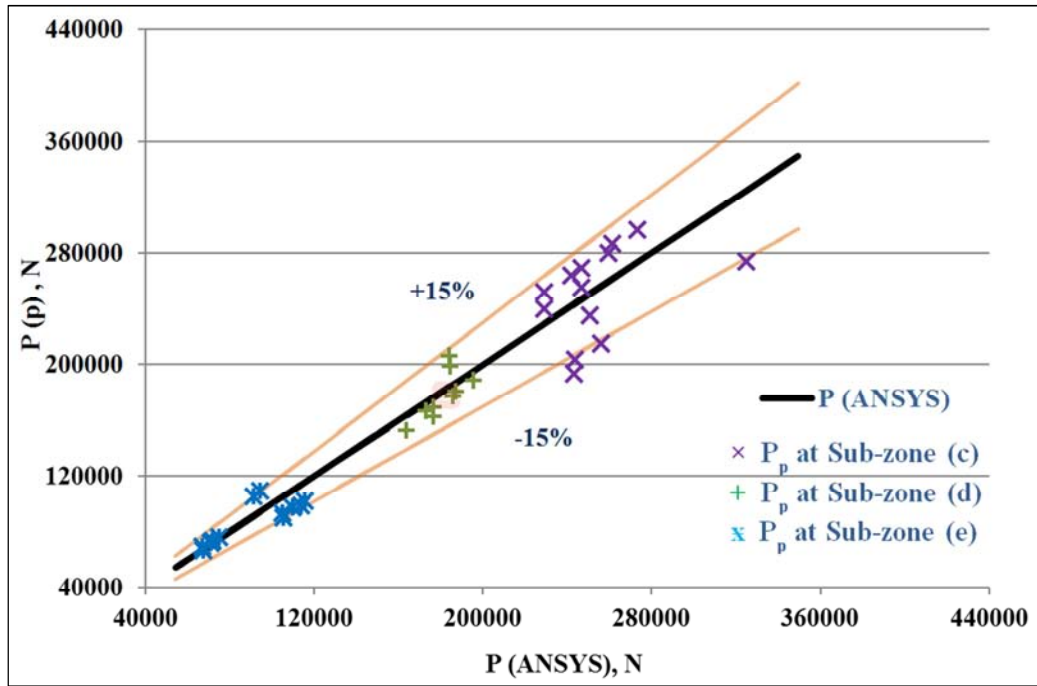


Figure 4. Results of ultimate load in zone (2).

5.3. Numerical Verification of Zone (3)

In this zone the column cross sections have different web depth to thickness ratio ( $b/t$ ) and the slenderness ratio ( $\lambda_x$ ) is more than 120. Most of the models are subjected to overall buckling and the rest is subjected to a combination of overall and another type of buckling. A comparison between results is presented in Figure 5.

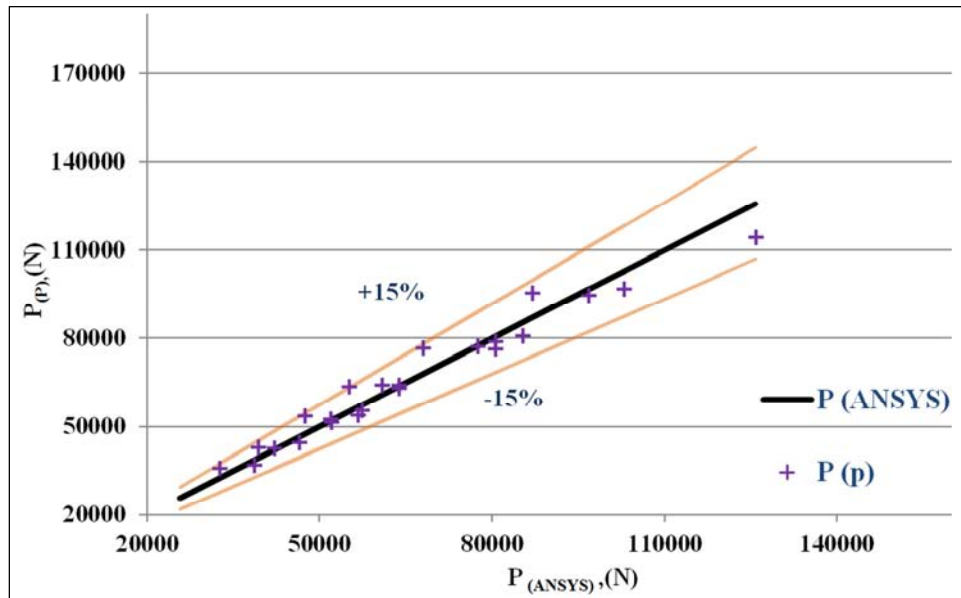


Figure 5. Results of ultimate load in zone (3).

6. Another Verification Method

Finite strip method (FSM) is one of the numerical methods, which is specially used for the prediction of the ultimate loads for members that have different cross sections [13]. The semi-analytical finite strip method is applied by using

CUFSM application [14]. FSM is used for all the previous specimens to estimate their ultimate loads. The comparison between the ultimate loads  $P_{(FSM)}$  obtained from FSM and the ultimate loads  $P_{(p)}$  obtained from proposed method is presented in Figure 6 to determine the accuracy of this method.

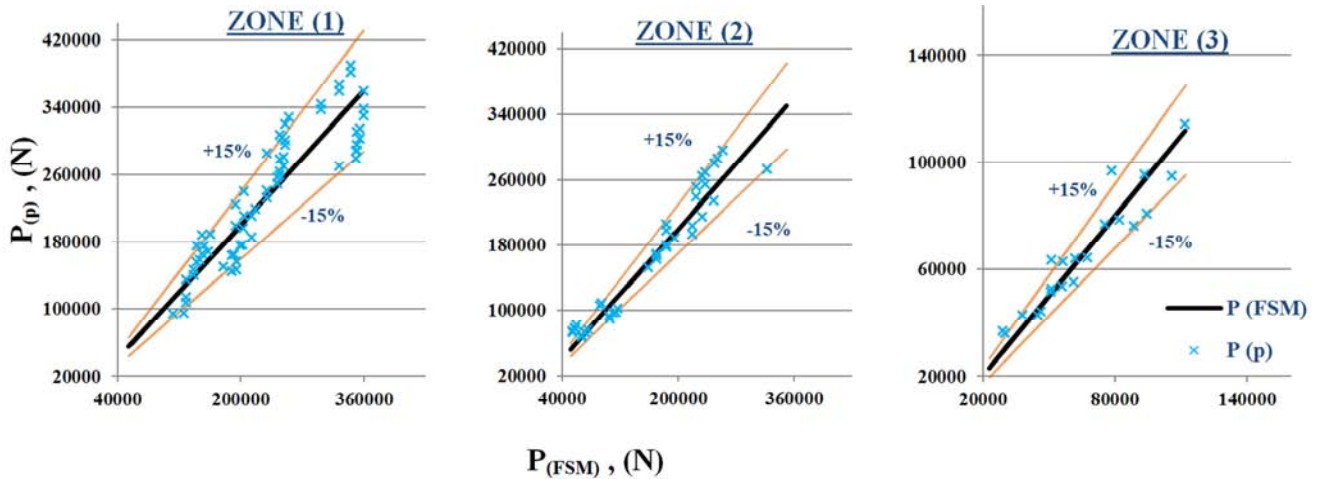


Figure 6. Comparison of results between FSM and proposed method.

### 7. Estimating Ultimate Loads for Double Lipped Channel Columns

The proposed method could be implemented in the case of double lipped channel columns. The different connection positions for back to back lipped columns have a big influence on the resulting buckling load. The three common connection positions are taken into consideration in this study as shown in Figure 7:

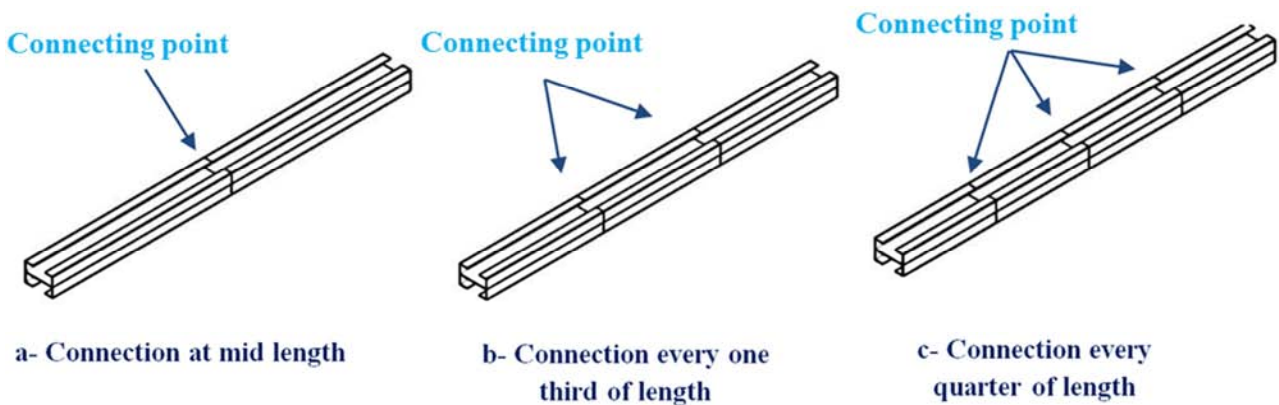


Figure 7. Different positions of connections.

The value of slenderness ratio ( $\lambda_x$ ) is depended on two main parameters, the unsupported length ( $L$ ) and radius of gyration ( $r$ ). The unsupported length for the columns changes depending on the place of the connections. As a result, the value of the slenderness ratio of column ( $\lambda_x$ ) changes to ( $\lambda_L$ ) as shown in Figure 8. The value of slenderness ratio ( $\lambda_L$ ) is then used when applying the proposed method.

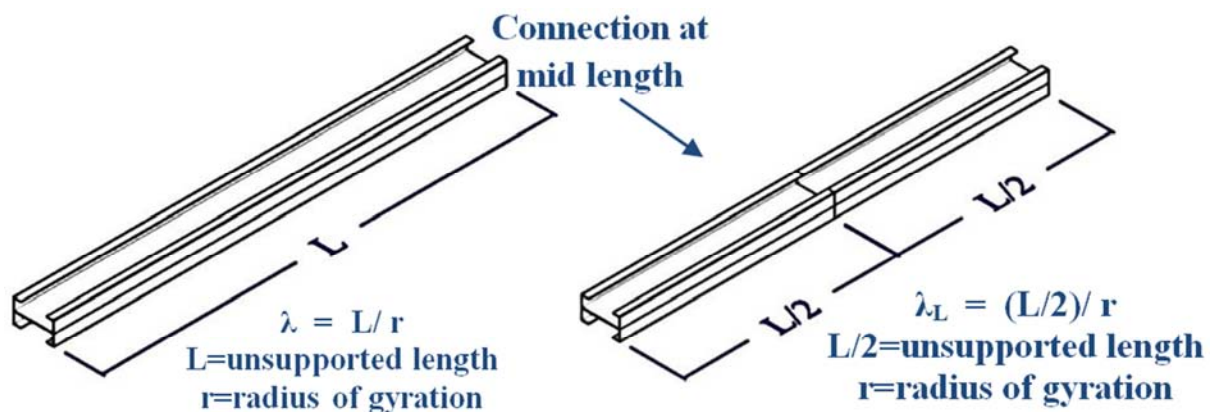


Figure 8. Overall and local slenderness ratio.

### 8. Application of Proposed Method on Columns with Different Connection Positions

A proposed method is applied to all columns in all zones and sub-zones to predict the ultimate loads. Based on the position of connection, the proposed method could be applied using the results of the slenderness ratio ( $\lambda_L$ ) and width to

thickness ratio (b/t).

Previous models were recalculated using different connection positions. According to the connection placement the values of slenderness ratio and web to depth ratio are changed. Table 3 illustrates some of the specimens that are connected back to back in three different positions. These specimens are chosen randomly.

Table 3. Specimens zones when connected in different placement.

Single Lipped channel				Back to Back Lipped channel											
Zone	Sub Zone	$\lambda_x$	b/t	Connected at mid length				Connected at third length				Connected at quarter length			
				Zone	Sub Zone	$\lambda_L$	b/t	Zone	Sub Zone	$\lambda_L$	b/t	Zone	Sub Zone	$\lambda_L$	b/t
1	a-2	68	80	1	a	34	40	1	a	23	40	1	a	17	40
1	b-1	39	100	1	a	20	50	1	a	13	50	1	a	10	50
1	a-7	48	71	1	a	24	35	1	a	16	35	1	a	12	35
1	b-34	61	125	1	a	31	62.5	1	a	20	62.5	1	a	15	62.5
2	e-5	96	150	1	a	48	75	1	a	32	75	1	a	24	75
2	d-1	71	100	1	a	36	50	1	a	24	50	1	a	18	50
2	e-4	92	150	1	a	65	75	1	a	43	75	1	a	33	75
2	d-23	97	140	1	a	48	70	1	a	32	70	1	a	24	70
2	c-1	78	71	1	a	39	36	1	a	26	36	1	a	20	36
3	23	156	83	2	c	78	42	1	a	52	42	1	a	39	42
3	29	167	56	2	c	83	28	1	a	56	28	1	a	42	28

The comparison between the ultimate loads  $P_{(ANSYS)}$  obtained from FEM and ultimate loads ( $P_p$ ) from the proposed methods for back to back lipped channel columns is presented for the different connection positions. The values of ultimate loads obtained from the proposed method vary about  $\pm 15\%$

from those obtained from the analytical FEM results. This comparison is presented as follow:

Figure 9 illustrates the comparison when the connection in the middle length.

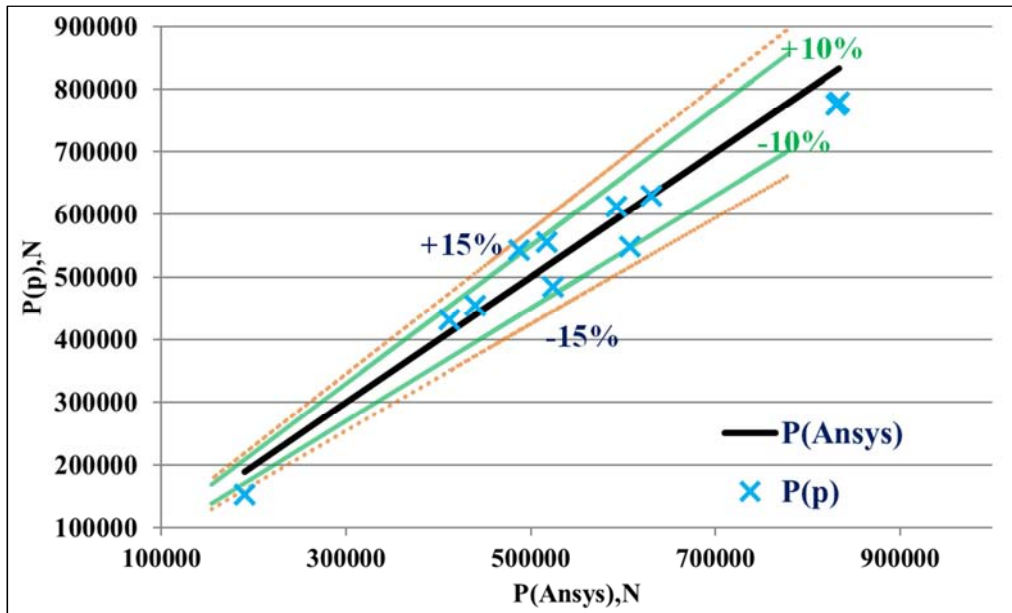


Figure 9. Comparison between  $P_{(Ansys)}$  and  $P_p$  in case of back to back lipped channel column connected at mid length.

Figure 10 shows the shape of buckling for Column (1). It consists of two lipped channels (Z1-a-26) back to back connected at mid length. The column is subjected to torsional buckling.

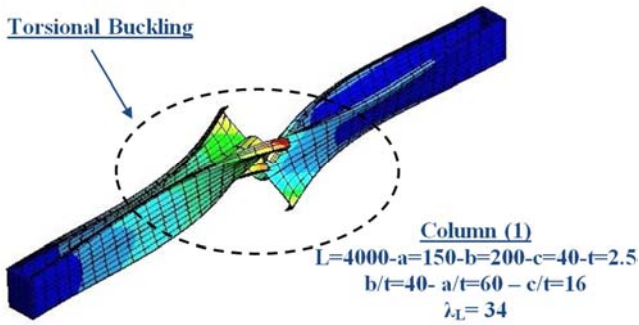


Figure 10. Buckling shape of column (1).

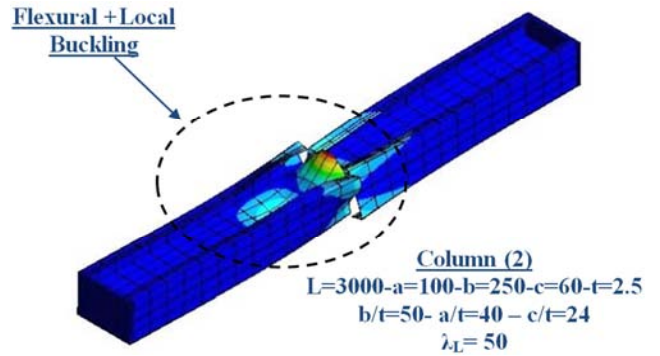


Figure 11. Buckling shape of column (2).

Figure 11 shows the shape of buckling for Column (2). It consists of two lipped channels (Z2-d-1) back to back connected at mid length. The lip and the flange of column are distorted at the connection with a wave of buckling in the web. As a result the buckling mode is characterized as Flexural + Local buckling.

Figure 12 illustrates the comparison when the connection in every third of length.

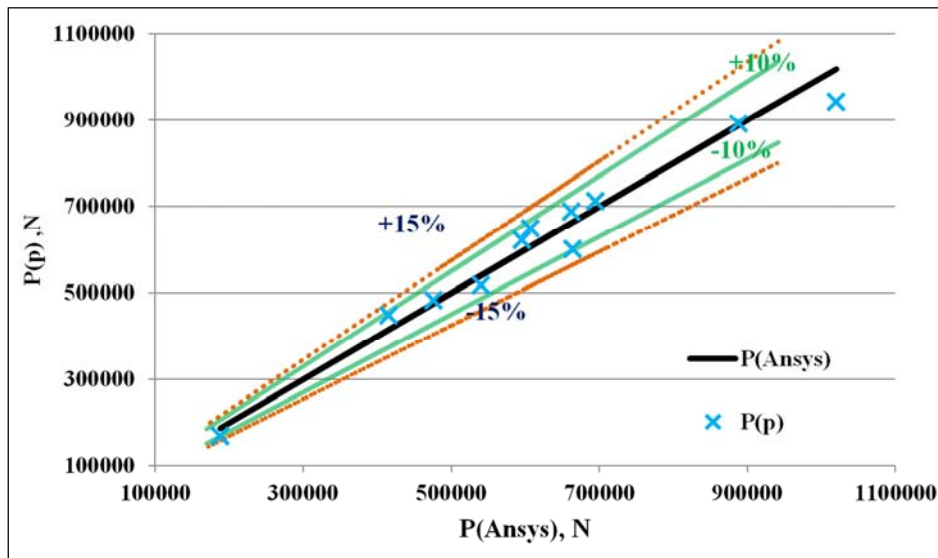


Figure 12. Comparison between  $P_{(Ansys)}$  and  $P_p$  in case of back to back lipped channel column connected at each third length.

Figure 13 shows the shape of buckling for column (3). It consists of two lipped channels (Z2-e-4) back to back connected at each third of the column's length. The column is subjected to distortional buckling due to the distortion of the lip and the flange at the connection without any change in the web.

Figure 14 shows the shape of buckling for column (4). It consists of two lipped channels (Z3-29) back to back connected at each third of column's length. The buckling mode is characterized as distortional buckling. The lip and the flange of this column are rotated at the connection with a wave of buckling in the web. As a result the buckling mode is characterized as Local + Distortional buckling.

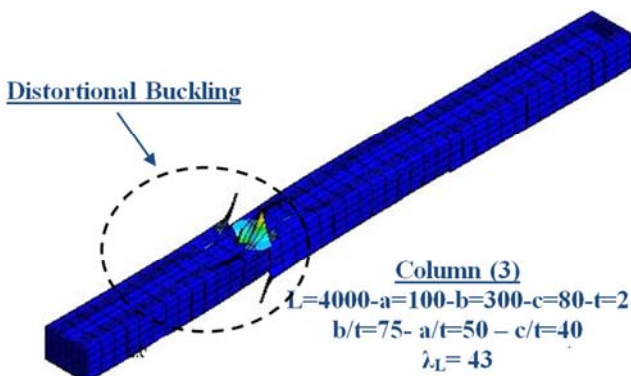


Figure 13. Buckling shape of columns (3).

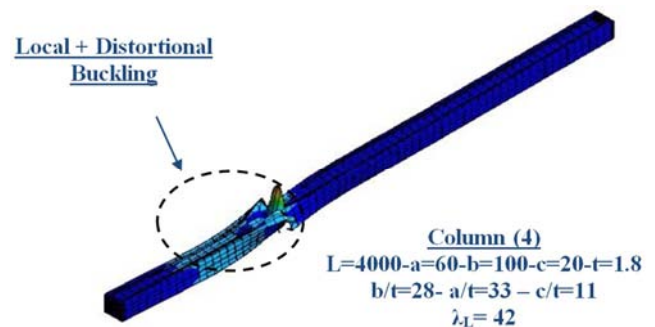


Figure 14. Buckling shape of columns (4).

Figure 15 illustrates the comparison when the connection in every quarter of length.

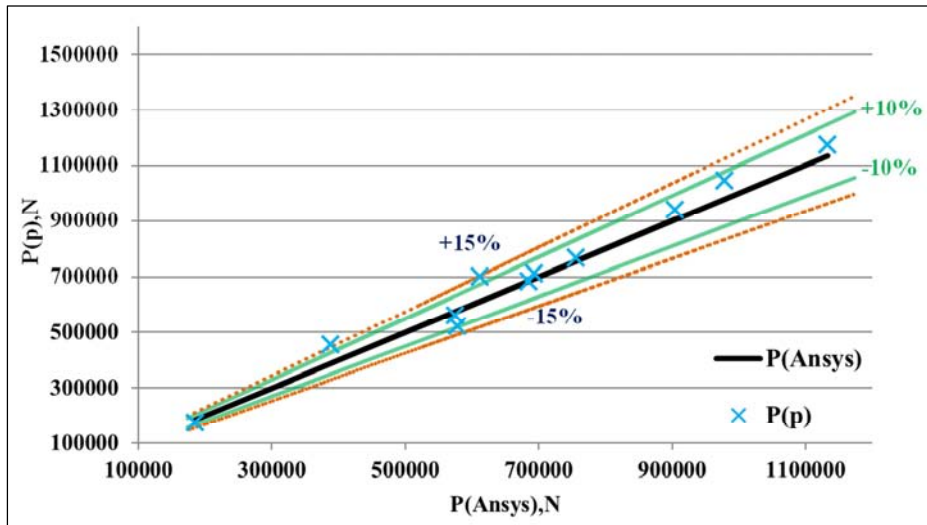


Figure 15. Comparison between  $P_{(Ansys)}$  and  $P_p$  in case of back to back lipped channel column connected at each quarter length.

Figure 16 shows the buckling behavior of column (5). It consists of two lipped channels (Z1-b-1) back to back connected at each quarter length. The lip undergoes bending with a little rotation of the flange at the connection without any deformation in the web. This buckling mode is characterized as Local buckling.

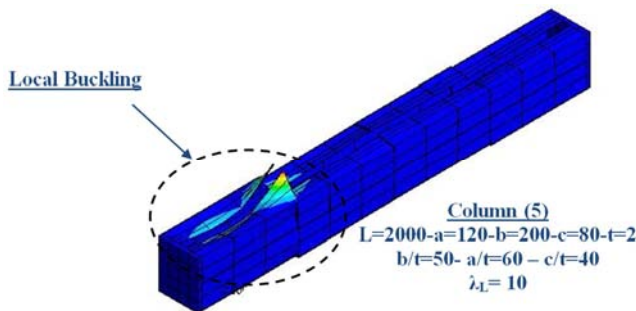


Figure 16. Buckling shape of columns (5).

Figure 17 shows the buckling behavior of columns (6). It consists of two lipped channels (Z3-23) back to back connected at each quarter length. The lip and the flange are distorted at the connection as well as the web. The buckling mode is characterized as Flexural + Flexural torsional buckling.

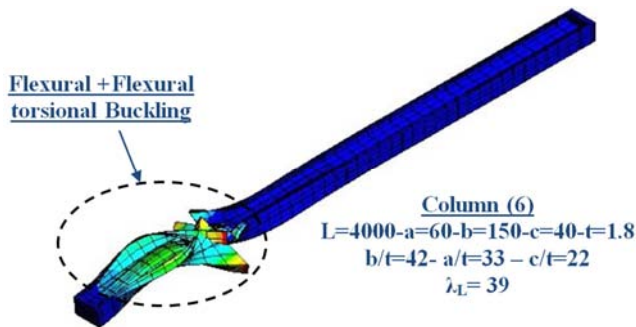


Figure 17. Buckling shape of columns (6).

### 9. The Condition for the Connections According to the Egyptian Code

The Egyptian specification code allows a limited spacing between connections in the case of built up sections that compose of two lipped channel. This spacing depends on the type of loading whether it is compression or tension. For compression members the longitudinal spacing between connections should be limited to the following value:

$$S_{max} = L * r_x / 2 * r_y \tag{2}$$

Where ( $S_{max}$ ) is the maximum longitudinal spacing, ( $L$ ) is the length of the compression member, ( $r_x$ ) is the radius of gyration of the section about the axis perpendicular to the direction in which buckling would occur and ( $r_y$ ) is the radius of gyration of one channel about the axis passes through the centroid which parallel to the web. The allowable spacing between connectors for the previous built up sections are estimated and presented in Table 4.

Table 4. Maximum distance between connectors.

Zone	Sub-Zone	L (mm)	$r_x$	$r_y$	$S_{max}$ (mm)
1	a-26	4000	59	86	1372
1	b-1	2000	52	78	667
1	a-7	3000	62	81	1148
1	b-34	3000	49	137	536
2	e-5	4000	42	117	718
2	d-1	3000	42	98	643
2	e-4	4000	44	115	765
2	d-23	4000	46	136	676
2	c-1	4000	52	78	1333
3	23	4000	26	58	897
3	29	4000	24	42	1143

It can be concluded from the values of ( $S_{max}$ ) for all previous built up specimens that the suitable positions of the connections according to the Egyptian specification code is

equal to (L/6) of total column length. Table 5 illustrates the change in the type of zones and sub-zones due to the place of the connection is at (L/6) of column length.

Table 5. Changing in zone due to connect at (L/6) of total length.

Single lipped channel				Back to Back Lipped channel			
Zone	Sub-Zone	$\lambda_x$	b/t	Zone	Sub-Zone	$\lambda_x$	b/t
1	a-26	68	80	1	a	8	40
1	b-1	39	100	1	a	7	50
1	a-7	48	71	1	a	12	35
1	b-34	61	25	1	a	10	62.5
2	e-5	96	150	1	a	16	75
2	d-1	71	100	1	a	24	50
2	e-4	92	150	1	a	15	75
2	d-23	97	140	1	a	16	70
2	c-1	78	71	1	a	13	36
3	23	156	83	1	a	37	42
3	29	167	56	1	a	28	28

Figure 18 shows the comparison between loads in case of back to back lipped channel columns connected at (L/6) of total column length.

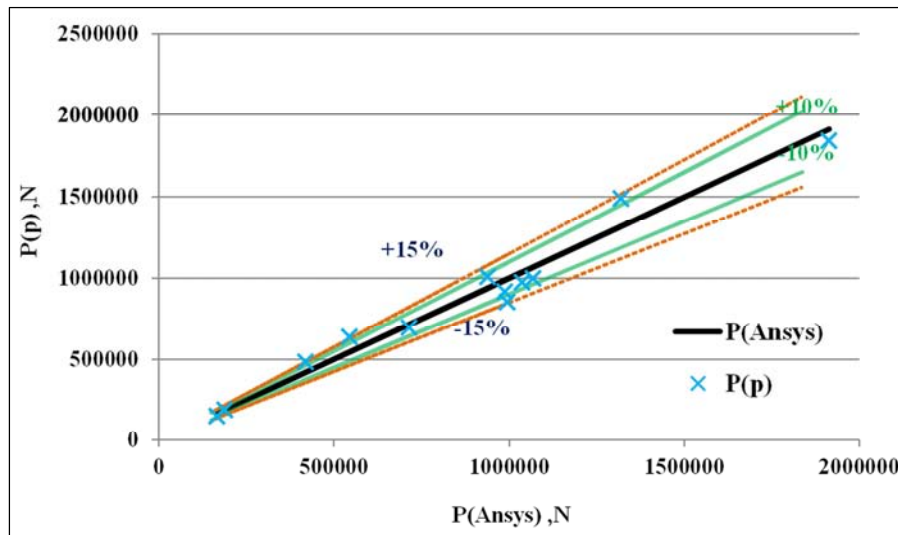


Figure 18. Comparison between  $P_{(Ansys)}$  and  $P_p$  in case of back to back lipped channel column connected at each (L/6) of total length.

### 10. Influence of Position Connections on Loads

Table 6. Ratio between ultimate loads for the different positions of connections.

Zone	FEM			Proposed method		
	$\frac{P_{(L/6)}}{P_{(L/2)}}$	$\frac{P_{(L/6)}}{P_{(L/3)}}$	$\frac{P_{(L/6)}}{P_{(L/4)}}$	$\frac{P_{(L/6)}}{P_{(L/2)}}$	$\frac{P_{(L/6)}}{P_{(L/3)}}$	$\frac{P_{(L/6)}}{P_{(L/4)}}$
1	2.01	1.74	1.5	1.74	1.56	1.36
1	2.3	1.88	1.69	2.37	1.95	1.57
2	1.59	1.49	1.35	1.91	1.67	1.42
2	1.24	1.14	1.1	1.4	1.32	1.22
2	2.03	1.49	1.45	1.69	1.53	1.34
2	1.36	1.32	1.24	1.42	1.34	1.23
2	1.68	1.64	1.62	1.4	1.32	1.22
2	1.7	1.61	1.41	1.58	1.45	1.3
3	1.02	1.01	1.08	1.1	1.06	1.05
3	1.01	1.01	1.02	1.03	1.11	1.08

Table 6 shows the comparison between the values of ultimate loads due to the change in the connection positions to emphasize the accuracy of results. This table illustrates the ratio between the value of ultimate loads when connected at (mid, third and quarter length) and at 1/6 of column length (according to Egyptian specification code). This comparison is between the ultimate loads obtained from FEM and ultimate load obtained from proposed method.

From the previous comparison it can be concluded that the values of ultimate loads depend on the place of connections in zones (1) and (2). The ultimate loads for columns that are connected at (L/6) could reach about 2.37% of those loads obtained from sections connected at mid length. The sections in zone (3) don't depend on the place of connection because they are subjected to overall buckling.

## 11. Conclusions

An extensive parametric study is performed to analyze the performance of 215 lipped channel columns under axial pure compression. The specimens are classified into three zones depending on the values of their slenderness ratio. Each zone is divided into sub-zones based on their web to depth ratio. A proposed method predicts the ultimate loads taking into account the previous parametric study. The concept of the proposed method is applied for all zones and sub-zones using different constants depending on the classification of the specimens. Ultimate loads obtained from the proposed method are compared to the ones obtained from FEM and they achieve a good match in all zones varying between  $\pm 15\%$ . Also the proposed method is applicable for columns that consist of 2-channels back to back. It's achieves ultimate load values about 90% of those obtained from FEM. The positions of connections between the two channels have a great influence on the column's ultimate load value. The values of ultimate loads aren't influenced by the place of connections in long columns of zone (3). Thus, the proposed method could be used to obtain reliable results quickly with less effort.

---

## References

- [1] Dr. Ahmed Shamel Fahmy and Eng. Rowida Saad Farrag, Simple proposal for estimating the ultimate load of cold-formed steel lipped channel columns, the ninth Alexandria international conference, December 2016.
- [2] <http://www.ansys.com/products>.
- [3] Martin Macdonald Muditha p. Kulatunga, Finite element analysis of cold formed steel structural members with perforations subjected to compression loading, school of engineering & built environment Glasgow Caledonian University Glasgow, UK, 2013.
- [4] Professor d.eng. Dan Dubina, Eurocodes background and applications, design of steel buildings with worked examples, Politehnica University Timisoara Romania.
- [5] Wei-Wen Yu, Cold-formed steel structures, department of civil Engineering, University of Missouri-rolla, rolla, 1999.
- [6] Thomas h.-K. Kang, Kenneth a. Biggs, and Chris Ramseyer, Buckling modes of cold-formed steel columns iacsit international journal of engineering and technology, vol. 5, no. 4, August 2013.
- [7] Rowida Saad Mohamed Farrag, Numerical investigation of the interaction of local and overall buckling of cold formed c-channel, July 2017
- [8] Ahmed Shamel Fahmy, Theoretische und experimentelle Untersuchungen zur Interaktion von Knicken und Beulen bei dünnwandigen kaltgeformten Bauteilen), Bauingenieur-und Vermessungswesen der Univesität Fridericiana zu Karlsruhe.
- [9] Mulligan, g. p, The influence of local buckling on structural behavior of singly symmetric cold formed steel columns, 1984.
- [10] Loughlan, J., Mode interaction in lipped channel column under concentric or eccentric loading.
- [11] Egyptian specifications, code no. (205), ministerial decree no 279-2001.
- [12] <https://www.ibm.com/analytics/us/en/technology/spss/spss-trials.html>.
- [13] Zhanjie Li Johns Hopkins, Buckling analysis of the finite strip method and theoretical extension of the constrained finite strip method for general boundary conditions, university 2009.
- [14] Professor Ben Schafer's, Thin-walled structures research group, Johns Hopkins University.